**AIR POLLUTION (H ZHANG AND Y SUN, SECTION EDITORS)**

# Evaluating the Impacts of Ground-Level O$_3$ on Crops in China

Hui Zhao[1,2,3] · Yuxin Zhang[4] · Qi Qi[1] · Hongliang Zhang[1,5]

## Abstract

China is facing increasing ground-level ozone (O$_3$) along with the reduction of particulate matter since the implementation of the Air Pollution Prevention and Control Action Plan (APPCAP) in 2013. High-level O$_3$ poses adverse effects to ecosystems by inhibiting the growth of crops and other plants in addition to human health effects. The capture of atmospheric carbon dioxide by plants is also weakened due to O$_3$ stress effect. In recent years, studies have been conducted to evaluate the potential risk of O$_3$ in agricultural production in China with different methods and focuses and the results are not consistent for comparison and policy-making. In this paper, we first briefly reviewed the levels of O$_3$ pollution in China in recent years, and the evaluation indicators for analyzing O$_3$ impacts on crops as well as their applicability. Then, methods for determining O$_3$ flux and the progress in dry deposition of O$_3$ in farmlands were presented. We also introduced some recent advances in evaluating losses of crop yield caused by O$_3$ exposure. Finally, in view of the shortcomings of current research, prospects for future research were suggested.

**Keywords** Ground-level O$_3$ · Crop damage · Flux · Dry deposition · Risk assessment

## Introduction

Ozone (O$_3$) in the stratosphere protects lives by effectively absorbing ultraviolet radiation from the sun, but ground-level O$_3$ produced by complex photochemical reactions of precursors such as nitrogen oxides (NO$_x$), volatile organic compounds (VOC$_S$), methane (CH$_4$), and carbon monoxide (CO) is harmful [1]. It has adverse effects on crops and natural vegetation in addition to human health. In the past few decades, due to the intensification of human activities, the emission of O$_3$ precursors has increased sharply, resulting in continuous increase of ground-level O$_3$ at a rate of 0.5–2% per year in the Northern Hemisphere [2]. Based on this upward trend, it is predicted that the average background O$_3$ concentration may reach 68 ppb by 2050, and even as high as 84 nL L$^{-1}$ in some areas by the end of this century [3–5]. Thus, it is crucial to evaluate and prevent adverse effects of O$_3$ using proper methods.

The current severe O$_3$ pollution in North America, Europe, and Asia is already sufficient to have negative effects on surface vegetation and food crops, including leaf damage, decline in photosynthesis, reduction in growth rate, changes in carbon distribution, closure of stomata, and premature aging [6–9]. If effective measures are not taken to curb the threat of O$_3$, it is estimated that the global O$_3$-induced yield losses of wheat, maize, and soybean in 2030 were 4.0–26.0%, 2.5–8.7%, and 9.5–19.0%, respectively [10], with total economic losses of \$12–\$35 billion each year. Therefore, an accurate assessment of the potential risks of O$_3$ to crops is not only the basis for implementation of air pollution prevention and control measures, but also

✉ Hongliang Zhang
zhanghl@fudan.edu.cn

1 Department of Environmental Science and Engineering, Fudan University, Shanghai 200438, China

2 Jiangsu Key Laboratory of Atmospheric Environment Monitoring and Pollution Control (AEMPC), Collaborative Innovation Center of Atmospheric Environment and Equipment Technology, Nanjing University of Information Science & Technology, Nanjing 210044, China

3 Guangdong Provincial Key Laboratory of Environmental Protection and Resources Utilization, Guangzhou Institute of Geochemistry, Chinese Academy of Science, Guangzhou 510640, China

4 School of Science, Hong Kong University of Science and Technology, Hong Kong 999077, China

5 Institute of Eco-Chongming (IEC), Shanghai 200062, China

an urgent need to improve the adaptability of China's food production to climate change and environmental pollution.

In recent years, with the rapid development of the national economy and the acceleration of industrialization and urbanization, China is facing the problem of regional air pollution characterized by high concentrations of $PM_{2.5}$ and $O_3$. In order to improve the current air pollution situation, China's State Council issued the Air Pollution Prevention and Control Action Plan (APPCAP) on September 10, 2013. Recent studies have suggested that the implementation of the APPCAP has significantly reduced the levels of $PM_{2.5}$ in eastern China [11, 12], but ground-level $O_3$ is becoming more and more serious, and it has replaced $PM_{2.5}$ as a new problem of air pollution in some large cities of China [12, 13]. China is a large agricultural country, and agriculture has always been the foundation of economic development. Studies have shown that ground-level $O_3$ that far exceeds the damage threshold of crops reduces crop growth and yield in China [5], thus seriously threatening food security. However, the evaluation methods are inconsistent and results are uncertain for policy-making to avoid the adverse effects of $O_3$.

Based on the above concerns, this paper focus on reviewing ground-level $O_3$ pollution and its potential risks to crops in China, and its structure is as follows: the "Overview of Ground-Level $O_3$ Pollution in China" section reviews the state of ground-level $O_3$ pollution in China; the "Indicators for $O_3$ Impacts on Crops" section systematically summarizes the development of $O_3$ risk assessment indices; the "Research Methods of $O_3$ Flux" section briefly introduces the methods of $O_3$ flux observation and stomatal uptake estimation; the "$O_3$ Dry Deposition in Farmland Ecosystem" section covers the dry deposition of $O_3$ in farmland ecosystem; the "Potential Risk Assessment of Ground-Level $O_3$ Pollution" section gives a detailed review of $O_3$ effects on crop yield; the "Limitations and Future Research Directions" section points out the shortcomings of the current research and provides suggestions for future researches. This review would provide a theoretical basis for the evaluation and control of $O_3$ pollution to avoid agricultural losses.

## Overview of Ground-Level $O_3$ Pollution in China

China's air pollution problem caused by rapid economic development and accelerated urbanization has become increasingly severe. China has also been committed to the monitoring and control of air quality over the past few decades. Since the 1980s, the China Meteorological Administration has established seven atmospheric background stations to conduct long-term monitoring of air quality [14], and thus, some early studies on $O_3$ pollution were limited to station observations due to the lack of large-scale $O_3$ data. For instance, ground-level $O_3$ was found to increase at a rate of 1.13 ppb per year during 2003–2015 at Shangdianzi station in Beijing and 1.80 ppb per year during 1991–2006 at Lin'an station in Zhejiang, respectively [15, 16]. A trend analysis of ground-level $O_3$ at the Waliguan station in Qinghai from 1994 to 2013 indicated that the growth rates during the daytime and nighttime were approximately $0.24 \pm 0.16$ ppb per year and $0.28 \pm 0.17$ ppb per year, respectively [17]. In the Pearl River Delta (PRD) region, Li et al. [18] reported that ground-level $O_3$ increased significantly from 2006 to 2011, with a mean trend of 0.86 ppb per year.

From January 2013, the Ministry of Ecology and Environmental of the People's Republic of China (MEE, PRC) had begun to publish hourly data of six air pollutants including $O_3$ in a web platform, which provided the researchers with a rare opportunity to analyze the distribution of $O_3$ on a regional scale based on observational data [19–21]. Figure 1 shows the spatial distributions of maximum daily 8-h average $O_3$ concentration (MDA8 $O_3$) during 2015–2020 in China. Overall, the high-level $O_3$ pollution was mainly concentrated in North China, Central China, and East China, which may be related to the high population density in these areas and the large amount of $O_3$ precursor emissions caused by frequent human activities [22]. The $O_3$ level in South China, Southwest China, and Northeast China was relatively low due to lower anthropogenic emissions and the influence of meteorological conditions [11]. Ground-level $O_3$ and its precursors like $NO_X$ and $VOC_S$ emissions present a complex non-linear relationship [15], and many previous studies have shown that the generation of $O_3$ depends on the ratio of $VOC_S/NO_X$ [1, 23, 24]. In general, in regions of high $NO_x$, reducing $VOC_S$ emissions could inhibit the production of $O_3$; however, higher $NO_x$ concentrations could also promote the formation of nitrous acid (HONO). HONO is one of the major contributors to the primary OH production in the troposphere. Its photolysis produces hydroxyl radical (OH) during the daytime, which enhances the atmospheric oxidation capacity, thereby increasing $HO_2$ and $RO_2$ concentrations leading to elevated $O_3$ concentrations [25, 26], as shown in reactions (1–11). Several studies have also confirmed that the increase in anthropogenic $VOC_S$ emissions was the main reason for the increase in $O_3$ concentration in eastern China [12, 14, 20]. Therefore, effective measures must be taken in the future to control $VOC_S$ emissions, thereby reducing ground-level $O_3$ pollution. In short, the production of $O_3$ is very complicated, affected by not only the emission of precursors and meteorological factors [14, 15], but also regional transport [11, 14].
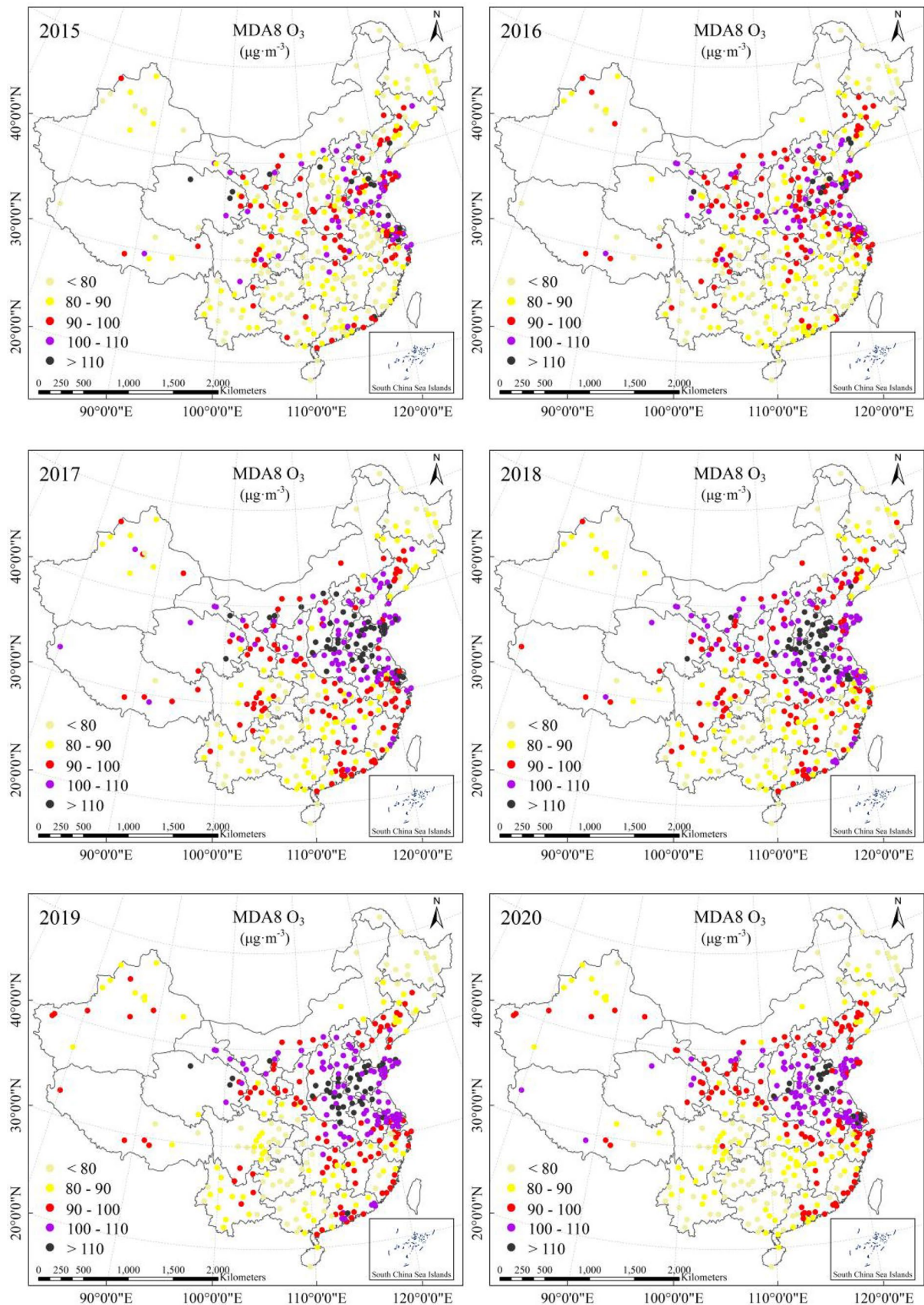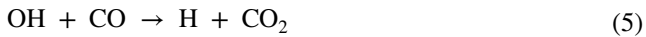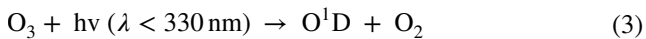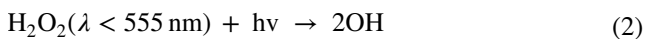
$$HONO + hv \ (\lambda < 400\,nm) \rightarrow NO + OH \quad (1)$$
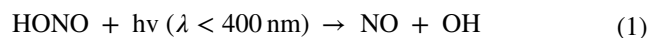
**Fig. 1** Spatial distributions of MDA8 O$_3$ during 2015–2020 across China

$$H_2O_2(\lambda < 555\ nm) + hv \rightarrow 2OH \tag{2}$$

$$O_3 + hv\ (\lambda < 330\ nm) \rightarrow O^1D + O_2 \tag{3}$$

$$O^1D + H_2O \rightarrow 2OH \tag{4}$$

$$OH + CO \rightarrow H + CO_2 \tag{5}$$

$$H + O_2 \rightarrow HO_2 \tag{6}$$

$$OH + VOC_S \rightarrow RO_2 \tag{7}$$

$$HO_2 + NO \rightarrow NO_2 + OH \tag{8}$$

$$RO_2 + NO \rightarrow NO_2 + RO \tag{9}$$

$$NO_2 + hv \rightarrow O + NO \tag{10}$$

$$O + O_2 \rightarrow O_3 \tag{11}$$

According to the method presented by Zhao et al. [11], five representative regions including Beijing-Tianjin-Hebei (BTH), Yangtze River Delta (YRD), Pearl River Delta (PRD), Chengdu-Chongqing (CC), and Fen Wei Plains (FWP) were selected to better understand the annual change characteristics of MDA8 $O_3$ in different regions, as shown in Fig. 2. On the whole, the annual mean MDA8 $O_3$ in BTH, YRD, and FWP were significantly higher than that in entire China (All). MDA8 $O_3$ exhibited an upward trend, from 85.7 µg m$^{-3}$ in 2015 to 95.1 µg m$^{-3}$ in 2017 for All, which may be associated with the decline in PM$_{2.5}$ due to the implementation of APPCAP (2013–2017) [12]. However, it experienced a significant decrease during 2018–2020,

reflecting the effectiveness of the implementation of the "Three-Year Action Plan to Win the Blue Sky Defence War" in China. It is noteworthy that MDA8 $O_3$ during 2015–2017 increased most rapidly with 31.8% increase from 78.0 to 102.8 µg m$^{-3}$ for FWP, followed by BTH (15.3% increase from 90.8 to 104.7 µg m$^{-3}$) and YRD (13.8% increase from 88.9 to 101.2 µg m$^{-3}$). From 2018 to 2020, CC had the largest MDA8 $O_3$ reduction (5.7% from 90.5 to 85.3 µg m$^{-3}$), whereas YRD only showed little reductions (1.5% from 99.0 to 97.5 µg m$^{-3}$).

## Indicators for $O_3$ Impacts on Crops

### Concentration- and Flux-Based Indices

Previous studies on $O_3$ impacts on crops are usually based on control experiments such as open-top chambers (OTC) and free air controlled exposure (FACE), both were conducted by setting different gradients of $O_3$ concentration to investigate the effects of $O_3$ on crop growth, photosynthesis, and yield. On the basis of these experiments, two indices were proposed to quantify the potential risks of $O_3$ to crops: concentration- and flux-based indices. Table 1 presents a brief summary of advantages and disadvantages of two metrics. In 1980, the U.S. Environmental Protection Agency (US-EPA) established the National Crop Loss Assessment Network (NCLAN), and researchers used OTC facilities to carry out experiments on the effects of $O_3$ on the growth and yield of wheat, rice, soybeans, maize, and other crops across the USA [27, 28]. These studies showed that there is a good linear relationship between the increase of $O_3$ concentration and the decrease of crop yield, and concentration–response relationships of different crops were established [3]. M7 and M12 are the most commonly used concentration-based exposure indices, which represent the average $O_3$

**Fig. 2** Inter-annual variations of MDA8 $O_3$ from 2015 to 2020 in different regions of China
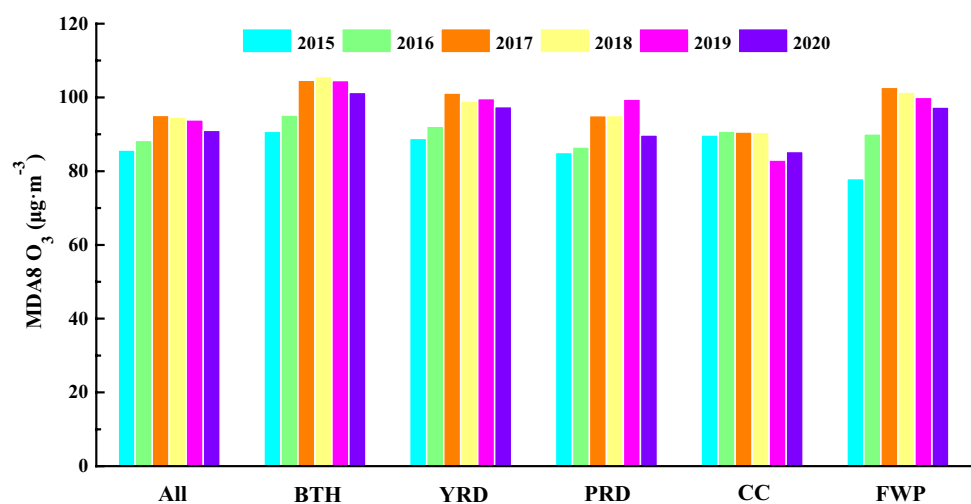
**Table 1** A comparison of different evaluation indices about the impacts of ground-level $O_3$ on crops

| Evaluation indices | Types and definitions | Advantages | Disadvantages |
|---|---|---|---|
| Concentration-based indices | M7: the average values of the hourly mean $O_3$ from 09:00 to 15:59 <br> M12: the average values of the hourly mean $O_3$ from 08:00 to 19:59 <br> SUM06: the sum of all hourly mean $O_3$ concentrations above 60 nL L$^{-1}$ <br> W126: a cumulative $O_3$ exposure indices according to sigmoidally weighted daytime $O_3$ concentrations <br> AOT40: the sum of hourly mean $O_3$ over a threshold of 40 ppb during the daytime | (a) Quick and simple calculation and easy to understand <br> (b) Less parameters requirements, and more widely used in $O_3$ risk assessment <br> (c) Only need to involve the $O_3$ concentration and/or exposure time | (a) No physical mechanism <br> (b) Only discuss the impact of $O_3$ on crops; the key environmental factors of crop growth are not considered <br> (c) Lack biological meaning |
| Flux-based indices | $POD_Y$: the accumulated stomatal $O_3$ uptake flux over a threshold of Y nmol m$^{-2}$ s$^{-1}$ | Climatic factors such as temperature, radiation, vapor pressure deficit, and soil moisture status that affect the stomatal conductance of crop leaves are considered | (a) Need to input too many parameters <br> (b) Complicated calculation process |

concentration for 7 h (09:00–15:59) and 12 h (08:00–19:59) during the growing seasons, respectively. The $O_3$ concentration–response relationships for crops are obtained by using mathematical statistics methods, and they are regarded as simple empirical relationships based on experiments. The calculation of M7 and M12 is relatively simple. However, these two indicators use $O_3$ concentration as the only influencing factor to reflect the response of crops to $O_3$ stress, and ignore the impacts of exposure time and crop growth condition [6], which cannot well reflect the actual damage effect of $O_3$ on crops.

With the deepening of the research, some researchers have realized that the negative effects of $O_3$ on crops have a cumulative effect [3]. Therefore, the US-EPA proposed SUM06 and W126 as plant protection standards in 1996. SUM06 refers to the hourly cumulative value of atmospheric $O_3$ concentration greater than 60 ppb. W126 represents the weighted accumulation of $O_3$ concentration during the daytime, which is calculated by multiplying the hourly $O_3$ concentration by weighting index, and then accumulating the value within a certain period of time. European researchers have pointed out that $O_3$ will cause injury to crops when it is higher than 40 ppb, and the $O_3$ exposure index AOT40 has a linear relationship with the reduction of crop yield [27]. Therefore, the AOT40 indicator is generally used as the standard for plant protection in Europe. This indicator is obtained by accumulating hourly mean $O_3$ over a threshold of 40 ppb during the daytime. In general, some cumulative exposure-based indices such as SUM06, W126, and AOT40 take into account not only the influence of $O_3$ concentration, but also the cumulative effect, and so they are more scientific than M7 and M12 [28].

$$M7(ppb) = \frac{1}{N} \sum_{i=1}^{N} [O_3]_i \tag{12}$$

$$M12(ppb) = \frac{1}{N} \sum_{i=1}^{N} [O_3]_i \tag{13}$$

$$SUM06(ppbh) = \sum_{i=1}^{N} [O_3]_i \text{ for } [O_3] \geq 60 \text{ ppb} \tag{14}$$

$$W126(ppbh) = \sum_{i=1}^{N} [O_3]_i \times W_i \tag{15}$$

$$AOT40(ppbh) = \sum_{i=1}^{N} ([O_3]_i - 40) \quad \text{for} [O_3] \geq 40ppb \tag{16}$$

where $N$ is the number of hours during crop growing seasons and $[O_3]_i$ is the hourly $O_3$ concentration in ppb. $W_i$ is the weighting index, and its calculation is as follows:

$$W_i = \frac{1}{1 + M \cdot \exp(-A \cdot [O_3]_i/1000)} \tag{17}$$

where $M = 4403$ and $A = 126$.

Some studies have shown that the impact of $O_3$ on crops is determined by the amount of $O_3$ that enters the crop body through the stomata of the leaves to undergo complex biochemical reactions [29–31], which is called the accumulated stomatal flux of $O_3$ ($POD_Y$), and its calculation is shown below in Eq. 18. The concentration-based exposure indices

like SUM06, W126, and AOT40 ignore the amount of $O_3$ absorbed by crop leaves through the stomata, and they default that the amount of atmospheric $O_3$ is equivalent to the amount of $O_3$ absorbed by the crop and does not involve the effect of stomatal conductance. On the one hand, when $O_3$ concentration in the ambient atmosphere is high, if the stomata resistance of the crop leaves is large, the $O_3$ absorption of the crop leaves would be low, and the damage caused by $O_3$ to crops will be greatly reduced [31]. On the other hand, there are also certain differences in the sensitivity of crops to $O_3$ under different crops, different growth periods of the same crop, and different environmental conditions. In addition, these indices do not take into account the crop's antioxidant capacity, detoxification capacity, and repair capacity at night, which may overestimate the negative effects of $O_3$ on crops [32]. Nevertheless, SUM06 and AOT40 are still widely recognized and applied.

$$POD_Y = \sum_{i=1}^{N} \max[F_{st} - Y, 0], \Delta t \tag{18}$$

where $F_{st}$ is the stomatal $O_3$ uptake flux in nmol $O_3$ $m^{-2}$ $s^{-1}$, $Y$ is the flux threshold, and $\Delta t = 1$ h [31].

Ground-level $O_3$ enters the terrestrial ecosystem through dry deposition, and then affects crop growth in the form of stomata absorption and non-stomata deposition. The stomata on the surface of crop leaves are the main channel for gas exchange with the outside world, which controls the photosynthesis and transpiration of crops. When the stomata are open during the daytime, $O_3$ enters the crop body through the stomata pathway. During the nighttime, the stomata are almost completely closed, and the amount of $O_3$ entering the crop body will be greatly reduced, or even close to zero. Studies have shown that the differences in the sensitivity of different types of crops to $O_3$ are determined by differences in stomata [33], so stomata play a very important role in the impact of $O_3$ on crops. Stomatal conductance indicates the degree of opening of stomata, and its size is related to the regulating effect of stomata. When the stomata resistance of the crop leaves is small and the stomata conductance is large, the amount of $O_3$ entering the crop will increase. Not only that, $O_3$ also affects the stomatal conductance, and many studies have found that $O_3$ can inhibits stomatal conductance, leading to an increase in stomatal resistance, thereby reducing stomatal $O_3$ flux [34]. The stomatal conductance model involves environmental factors such as phenological period, temperature, light intensity, water vapor pressure difference, and soil moisture content, and its simulation is often based on the Jarvis model and the Ball-Berry model [35–37]. Stomatal $O_3$ absorption flux is determined by the stomatal conductance and $O_3$ concentration, and therefore, the relationship between them has become an important issue in this field.

## Determination of Damage Thresholds for $O_3$

A few studies have shown that crops have certain defense and detoxification capabilities against $O_3$ stress. The antioxidants such as ascorbate in the cell wall can remove a small part of $O_3$ that enters the body of the crop [29]. Therefore, both concentration-based indices and flux-based indices have a damage threshold, which is an empirical value reflecting the negative effects of $O_3$ on crops, meaning that the impact below this empirical value is negligible. For example, 60 ppb, 40 ppb, and $Y$ represent the threshold values of SUM06, AOT40, and $POD_Y$, respectively [38]. In fact, the threshold $Y$ in $POD_Y$ varies with crop types, growth periods, crop varieties, and environmental factors. So far, there is no model that can completely describe the dynamic process of $Y$; the only way to determine the threshold $Y$ is to establish the relationship between $POD_Y$ and crop yield loss. The calculated cumulative stomatal $O_3$ absorption flux had the highest correlation with the relative yields of wheat and potato in European when the threshold $Y$ is set to be 6 nmol $m^{-2}$ $s^{-1}$ [29]. A flux threshold of 2 nmol $m^{-2}$ $s^{-1}$ was judged as a reasonable for an $O_3$ flux-based response relationship for rice in the Pearl River Delta of South China [39]. Feng et al. [40] proposed that the strongest relationship was found by using the $O_3$ uptake threshold of 12 nmol $m^{-2}$ $s^{-1}$ for winter wheat in subtropical China. Wu et al. [31] found that $POD_{4.0}$ (the accumulated stomatal $O_3$ flux over a threshold of 4.0 nmol $m^{-2}$ $s^{-1}$) had the best linear correlation with the relative yield of winter wheat in the Yangtze River Delta, which was consistent with the results of Tong et al. [41], but lower than those reported in European studies [29, 35]. Zhang et al. [42] reported that the $O_3$ absorption flux threshold of 9.6 nmol $m^{-2}$ $s^{-1}$ was most reasonable for soybean flux-response relationship in Northeast China.

To sum up, the threshold used for crop yield loss assessment using flux-based indices was set as a constant in the previous studies. Therefore, taking the detoxification effect of crops into account in the $O_3$ risk assessment model can provide a strong basis for accurately predicting crop yield losses.

## Applicability of Different Evaluation Indices

A large number of experiments on the effects of $O_3$ on crops showed that flux-based exposure indices provided stronger relationships with the damage effect of crops than concentration-based exposure indices such as AOT40 [5]. An experiment conducted in Europe showed the relative yields of wheat and potato had a stronger correlation with the stomatal $O_3$ flux indices than with AOT40 indices [43]. The study of Karlsson et al. [44] also confirmed that the stomatal $O_3$ flux was more closely correlated with visible foliar $O_3$ injury in Southern European forests than AOT40.

Goumenaki et al. [45] suggested that the performance of stomatal $O_3$ flux as a descriptor of $O_3$ risk to lettuce was better than the performance of AOT40 in Europe. Mills et al. [30] collected and analyzed studies on the potential ecological risks of $O_3$ in 17 European countries in the past 20 years and concluded that stomatal $O_3$ flux was better than AOT40 as an index of $O_3$ risk assessment for vegetation. In China, Feng et al. [40] developed and parameterized Jarvis-type stomatal conductance model for winter wheat and used it to establish the relationship between stomatal $O_3$ flux and yield loss. A rice experiment conducted in the Pearl River Delta region of China indicated that the accumulated stomatal $O_3$ uptake flux had a strong negative linear relationship with the relative yield, and its correlation coefficient was higher than that of the AOT40 index [39], whereas in wheat experiments of the North China Plain, both AOT40 and stomatal $O_3$ uptake flux were found to have a good relationship with relative yield [41], which was similar to the study by Gonzalez-Fernandez et al. [46].

## Research Methods of $O_3$ Flux

As mentioned above, $O_3$ flux-based index is the future research directions as it can better describe the impact mechanism of $O_3$ on crops than $O_3$ concentration-based index, and thus, the observation and simulation of $O_3$ flux in farmland ecosystems are a prerequisite for accurately implementing $O_3$ risk assessment for agricultural crops. The following introduces some research methods of $O_3$ flux.

### Flux Chamber Method

The flux box method is regarded as a traditional method to directly measure the gas exchange of plants. There are two types of flux chambers: static (closed, passive) and dynamic (flow-through, active) [47]. Among them, the static chamber method is the most widely used experimental measurement method. During the measurement process, a chamber is used to cover the measured crop, and the contact port between the chamber and the base is sealed with water to ensure that the air in the chamber does not have any exchange with the outside world. The gas concentrations in the chamber are measured at a certain time interval, and then, the following formula is used to calculate the gas exchange flux:

$$F_g = h_c \times \frac{M_g \times P}{R \times T} \times \frac{\partial_c}{\partial_t} \tag{19}$$

where $F_g$ is the gas flux (mg m$^{-2}$ h$^{-1}$), $h_c$ is the height of the chamber (m), $M_g$ is the molar mass of the gas (g mol$^{-1}$), $P$ is the air pressure (Pa), $R$ is the universal gas constant ($R = 8.3144$ Pa m$^3$ mol$^{-1}$ K$^{-1}$), $T$ is the temperature (K), $c$

is the gas volume fraction in the chamber ($\times 10^{-9}$), and $t$ is the time for the chamber to cover the measured crop (s). The static chamber method has the advantages of simple principle, easy operation, and low cost, but its disadvantages are that the natural turbulent state of the air on the surface of the measured crop is changed, which affects the measurement of exchange flux to a certain extent [48].

The dynamic chamber is an open system, its working principle is that the opposite sides of the chamber are opened so that a certain flow of air can pass through the chamber, and then, the gas exchange flux can be obtained by measuring the inlet and outlet concentration of the gas. The calculation method is as follows:

$$F_g = Q \times \rho_g \times \frac{C_1 - C_2}{A} \tag{20}$$

where $Q$ is the flow rate of the gas in the chamber (m$^3$ h$^{-1}$), $\rho_g$ is the gas density (g m$^{-3}$), and $C_1$ and $C_2$ are the outlet and inlet concentrations of the gas, respectively (mL L$^{-1}$). $A$ is the basal area of the chamber (m$^2$). When this method is used to measure the gas exchange flux, it is necessary to minimize the difference of air pressures between inside and outside of the chamber to avoid the gas flowing into or out of the chamber through the gap, which can affect the accuracy of the measurement results. In general, it is very accurate and reliable to use the dynamic chamber method to measure gas exchange flux. However, the equipment required to perform the measurements is expensive and the operation is more complicated. Although the static box method has certain drawbacks, it can realize continuous monitoring and is very easy to operate, so it has been widely used so far.

### Model Simulation Method

Previous studies on $O_3$ flux using flux chamber method are mostly based on controlled and semi-controlled experiments, and are limited to specific study areas, which consumes a lot of manpower and material resources. The model simulation method can overcome the above shortcomings very well and can be used to describe the entire change process, but this method is mainly applied to the stomata $O_3$ absorption flux on the leaf scale. There are many models that can estimate the stomata $O_3$ flux, among which the Jarvis-type multiplicative stomatal conductance model is the most commonly used [38], which is calculated by multiplying the leaf stomatal conductance and the $O_3$ concentration [29]:

$$g_{sto} = g_{max} \times \min(f_{phen}, f_{O_3}) \times f_{PAR} \times \max\left[f_{min}, (f_{temp} f_{VPD})\right] \tag{21}$$

where $g_{sto}$ is the calculated value of stomatal conductance of $O_3$ (mmol m$^{-2}$ s$^{-1}$), $g_{max}$ is the maximum value obtained from a large number of observations of stomatal

conductance (mmol m$^{-2}$ s$^{-1}$), $f_{min}$ is the minimum relative stomatal conductance, the factors $f_{phen}$, $f_{O_3}$, $f_{PAR}$, $f_{temp}$, and $f_{VPD}$ are expressed as the adjustment coefficients of phenology, $O_3$, radiation, temperature, and VPD (vapor pressure deficit) to $g_{max}$, and their values are between 0 and 1. The continuous stomatal conductance can be calculated by using the observed hourly climate and environmental factor data, and finally, the following formulas can be used to estimate the stomatal $O_3$ absorption flux:

$$F_{st} = \frac{[O_3]}{r_b + r_c} \times \frac{g_{sto}}{g_{sto} + g_{ext}} \tag{22}$$

$$r_b = \frac{1}{g_b} = \frac{1}{0.125 \cdot \left(\sqrt{\frac{u}{w}}\right) \times 1000} \tag{23}$$

$$r_c = \frac{1}{g_{sto}} \tag{24}$$

where $F_{st}$ is the leaf stomata $O_3$ flux (nmol m$^{-2}$ s$^{-1}$), $[O_3]$ is $O_3$ concentration, $g_b$ is the leaf boundary layer conductance (mmol m$^{-2}$ s$^{-1}$), $g_{ext}$ is usually set to be 16.4 mmol m$^{-2}$ s$^{-1}$, $u$ is the wind speed at canopy height (m), and $w$ is the maximum width of leaf (m). It is necessary to determine the parameter values in the stomatal conductance model before calculating the stomatal $O_3$ absorption flux. The model simulation method can predict the stomatal $O_3$ uptake flux of crop leaves in different regions, and thus, further research is needed to combine atmospheric models or satellite remote sensing methods to extend it to the regional scale.

## Micrometeorological Method

The gradient method and the eddy correlation method are micrometeorological methods for observing the $O_3$ flux in the terrestrial ecosystem. When using the gradient method to measure $O_3$ flux, two (or multiple) layers' observations of $O_3$ concentration, wind speed, and temperature should be implemented, and then, the near-surface turbulent flux is calculated by flux-profile relationship [9]:

$$F_o = K_o \times \frac{\partial \rho_o}{\partial z} \tag{25}$$

where $K_o$ is the turbulent exchange coefficient for $O_3$ (m s$^{-1}$), and its calculations refer to the study of Wu et al. [48]. $\partial \rho_o / \partial z$ is the vertical gradient of $O_3$ concentration with height $z$ (μg m$^{-3}$). Since the absolute concentration of $O_3$ is very low and the concentration gradient is relatively small, the calculation of $O_3$ flux by this method requires high-precision instruments and suitable meteorological conditions.

It should be noted that the eddy correlation method is regarded as an advanced method for measuring the atmospheric $O_3$ flux over terrestrial ecosystems in recent years, and it has been applied in the observation of $CO_2$ and water vapor flux [49]. However, it is almost still in a blank state in the application of $O_3$ flux. The calculation formula of $O_3$ flux is as follows [38]:

$$F_o = -\overline{\rho_o} \times V_d = \rho_o \times \frac{\overline{w' S'_o}}{\overline{S_o}} \tag{26}$$

where $V_d$ is deposition velocity, $\rho_o$ is the absolute concentration of $O_3$ observed by the slow-response $O_3$ analyzer, $w$ is the vertical wind speed (m s$^{-1}$), $S_o$ is the the signal output of the fast response $O_3$ analyzer, the upper horizontal line represents the time average, and the apostrophe represents the pulsation of the variable. Similar to the calculation of eddy covariance fluxes of $CO_2$ and water vapor, the observed $O_3$ flux also undergoes a series of corrections (coordinate rotation correction, spectrum correction, the Webb-Pearman-Leuning correction, etc.) and quality control [38].

# $O_3$ Dry Deposition in Farmland Ecosystem

## Processes and Its Influencing Factors

The terrestrial ecosystem is one of the important sinks of ground-level $O_3$. Because $O_3$ is difficult to dissolve in water, it enters the terrestrial ecosystem through dry deposition [50]. In recent years, a large number of studies have been conducted on the dry deposition characteristics of ground-level $O_3$ in forests, crops, and grasslands [51–57]. In general, $V_d$ is used to study the deposition law of $O_3$ in different ecosystems. The change of $V_d$ is largely controlled by the physiological activity of vegetation and meteorological factors, and the $V_d$ of different underlying surfaces is very different. The dry deposition of $O_3$ is affected by environmental factors such as wind speed, temperature, humidity, solar radiation, and soil moisture content. Under moderate or strong solar radiation, when the soil moisture is higher and the water vapor pressure difference is lower, the $V_d$ is greater [57]. Studies have pointed out that the threshold value of soil moisture is 12–13%, and $V_d$ will be reduced when it is lower than this threshold [58–60]. Thus, the value of $V_d$ is greater in the rainy season and humid conditions, which is because the soil water use efficiency is greater during this period [61–63]. Kurpius et al. [64] showed that VPD is the most important factor affecting $V_d$, and has a negative correlation with $V_d$. Zhu et al. [65] reported that the dry deposition process of $O_3$ is most significantly affected by solar radiation and relative humidity, and is positively correlated with relative humidity [66]. In addition, wind speed, atmospheric

stability, and friction velocity also have a strong correlation with $V_d$, indicating that the dry deposition process of $O_3$ is largely controlled by dynamics [67].

Due to the influence of meteorological conditions, $V_d$ presents the obvious diurnal variation characteristics. For farmland ecosystems, $V_d$ during the day is higher than that at night [54]. For example, Zhu et al. [65] used the eddy correlation method to observe the $V_d$ over a summer maize field in Northwestern Shandong Plain of China and found that the average $V_d$ during daytime and nighttime were 0.29 cm s$^{-1}$ and 0.09 cm s$^{-1}$, respectively, and the maximum value of $V_d$ was 0.81 cm s$^{-1}$ at 12:30. In the $V_d$ observations over winter wheat fields based on the gradient method in Nanjing, Li et al. [68] reported that the average values of $V_d$ during the entire observation period were 0.71 cm s$^{-1}$ during daytime and 0.40 cm s$^{-1}$ during nighttime. $V_d$ is related to the activity of photosynthesis, because the stomatal conductance is higher when the activity of photosynthesis is stronger. An observation experiment based on the eddy correlation method over a bare soil in Nanjing area in autumn showed that during the observation period, $V_d$ began to rise at about 03:00, reached the maximum at about 08:00, and then gradually decreased [69]. It should be noted that $V_d$ also changes with the advancement of crop growing period. Generally, $V_d$ reaches the maximum during the period from the flowering stage to the filling stage of wheat [70]. Because photosynthesis is the strongest during this period, when the stomata are opened for photosynthesis, $O_3$ is also easy to enter the stomata, and then, $V_d$ gradually decreases due to the senescence of leaves [64, 71, 72].

### Distinction of Total $O_3$ Flux

Several studies have shown that $O_3$ deposition can be divided into stomata absorption and non-stomatal deposition pathways, and the non-stomatal deposition includes soil and cuticular depositions. It must be pointed out that the chemical reaction of $O_3$ with NO and VOC$_S$ derived from the soil and leaves is another channel for $O_3$ deposition [73]. Currently, it is difficult to continuously observe stomatal $O_3$ absorption flux due to the difficulty of monitoring, and thus, it is usually estimated by stomatal resistance model. In addition, non-stomatal deposition cannot be directly observed, and research on it is mainly based on model methods. There are differences in the proportion of stomatal absorption in the total $O_3$ flux in different growth periods of crops. In China, this proportion during the peak growth period of winter wheat is less than 50–60%, and it gradually decreases during the aging process of wheat leaves [74], which is consistent with the observations of wheat, barley, and onion in Italy [75, 76], whereas in the vigorous growth period of potatoes, it is about 85%, and it decreases to about 20% during the maturity stage. Zhao et al. [77] observed $O_3$ flux in

rice fields using the eddy correlation method and used the revised Jarvis stomatal conductance model to distinguish its contribution to different deposition channels and found that the proportions of stomatal $O_3$ absorption and non-stomatal flux to total $O_3$ flux were 34.0% and 66.0%, respectively, and the proportions during the daytime were 49.0% and 51.0%, respectively. A comparison of $V_d$ during the daytime and the nighttime by Zhu et al. [65] indicated that stomatal $O_3$ absorption during the daytime was the main sink of atmospheric $O_3$ over maize field.

## Potential Risk Assessment of Ground-Level $O_3$ Pollution

Ground-level $O_3$ pollution and its potential risks to crops have received extensive attention in recent years. Although many studies have evaluated the impact of $O_3$ pollution on crop growth and yield in China, exposure–response relationships used in these studies are mainly based on experiments conducted in Europe and the USA due to the lack of field experiments. In view of differences in climatic conditions and crop varieties, the response of crops to $O_3$ stress in different regions may also be significantly different [78], and thus, there may be some possible limitations when applying external exposure–response relationships to analyze the impact of $O_3$ on crops in China. In order to improve the accuracy of the evaluation results, some researchers have carried out experiments on the effects of elevated atmospheric $O_3$ concentration on crops using OTC and FACE facilities in China [31, 42, 79, 80], and established the relationship between the relative yields of different crops and $O_3$ risk assessment indicators (Table 2), which provides an excellent opportunity for researchers to quantify the local and regional effects of ground-level $O_3$ on crop yields under past, current, and future.

In China, previous studies on crop yield reduction caused by ground-level $O_3$ pollution are usually based on $O_3$ data from a limited number of monitoring sites, satellite data, and model simulation results [85–88]. At the site scale, the $O_3$-induced yield losses of wheat and rice in Chongqing during 1990–1995 were 0.2–9.8% and 1.1–5.8%, respectively, using the AOT40 and M12 metrics, and those in 2020 were 12.0% and 10.8%, respectively [89]. In the Northwest Shandong Plain of China, the high level of ground-level $O_3$ was estimated to induce the yield loss of 12.9% for winter wheat based on AOT40 index [90]. Due to the lack of observational data, previous studies on regional-scale $O_3$ risk assessment mainly relied on simulated $O_3$ concentrations from atmospheric chemistry models or satellite data [91]. On the basis of the WRF/Chem-CHASER model, the $O_3$-induced yield loss for wheat ranged from 6 to 15% for the whole China [88], whereas in 2014, ground-level $O_3$ was

**Table 2** A summary on the response relationship between crop yield and $O_3$ evaluation index in China

| Crop | Cultivars | Sites | Facility | Years | Dose–response | References |
|---|---|---|---|---|---|---|
| Wheat | Jingdong 6 | Dingxing | OTC | 1999 | $RY = 1 - 0.0130 AOT40$ | [79] |
| | Yangmai 185, Jia 002 | Jiaxing | OTC | 2004–2008 | $RY = 1 - 0.0228 AOT40$ | [80] |
| | Yannong 19, Yangmai 16, Yangmai 15, Yangfumai 2 | Jiangdu | FACE | 2006–2009 | $RY = 0.961 - 0.0250 AOT40$ $RY = 0.994 - 0.2030 POD12$ | [40] |
| | Beinong 9549 | Changping | OTC | 2010 | $RY = 1 - 0.0170 SUM06$ $RY = 1 - 0.0220 AOT40$ $RY = 1 - 0.0370 POD4$ | [41] |
| Rice | Zhongzuo 9321 | Dingxing | OTC | 1999 | $RY = 1 - 0.0053 AOT40$ | [79] |
| | Jiahua 1 | Dingxing | OTC | 2004 | $RY = 1 - 0.00526 AOT40$ | [81] |
| | Jiahua 2, Fan 3694 | Jiaxing | OTC | 2004–2008 | $RY = 1 - 0.0095 AOT40$ | [80] |
| | Shanyou 63, Wuyujing 003 | Jiangdu | FACE | 2007 | $RY = 1 - 0.0160 AOT40$ | [82] |
| | Wuyunjing 15, Yangdao 6, Shanyou 63, Liangyou-peijiu | Jiangdu | FACE | 2007–2009 | $RY = 0.969 - 0.022 AOT40$ $RY = 0.998 - 0.078 POD11$ | [83] |
| | Yuejingsimiao 2 | Dongguan | OTC | 2009 | $RY = 1 - 0.0240 SUM06$ $RY = 1 - 0.0390 AOT40$ $RY = 1 - 0.0230 POD2$ | [39] |
| Maize | Zhengdan 958 | Yanqing | OTC | 2018 | $RY = 1 - 0.00577 AOT40$ $RY = 1 - 0.0426 POD6$ | [84] |
| Soybean | Hefeng 55, Heinong 35, Heinong 37, Suinong 22 | Harbin | OTC | 2013–2014 | $RY = 1 - 0.0074 W126$ $RY = 1 - 0.0066 SUM06$ $RY = 1 - 0.0120 AOT40$ $RY = 1 - 0.0540 POD9.6$ | [42] |

projected to cause the yield losses of 8.5–14.0%, 2.2–5.5%, and 3.9–15.0% for winter wheat, maize, and rice, respectively [92]. In the future projection, Tang et al. [93] used the CTM model to simulate the spatial distribution of AOT40 and stomatal $O_3$ flux for rice across China, and concluded that the $O_3$ risk for single rice, double-early rice, and double-late rice increased by 162–412% from 2000 to 2020. The crop yield losses due to $O_3$ exposure for the year 2030 were also estimated to be 19.7–25.7% for wheat and 5.8–7.9% for maize according to CTM model simulation [10].

In recent years, the MEE, PRC has established ambient air quality monitoring sites in almost all cities in China. The measured $O_3$ data can not only truly reflect the status of $O_3$ pollution, but also improve the accuracy of $O_3$ risk assessment [87]. Therefore, evaluating regional-scale $O_3$ agricultural risks based on observational $O_3$ data has already been used in some recent studies. In the Yangtze River Delta of China, ground-level $O_3$ in 2015 was estimated to induce the yield losses of 9.9–36.1% for wheat and 7.3–23.9% for rice [78], whereas in the study by Ren et al. [94], the yield losses of wheat and rice during 2014–2019 were 4.9–11.4% and 9.4–19.3%, respectively. In the southern region of China, the $O_3$ concentration in 2015 caused an estimated yield loss in rice of 1.2–10.4% [95]. In the North China Plain, the $O_3$-induced yield losses during 2014–2017 ranged from 6.4 to 38.2% for wheat and from 8.2 to 13.4% for maize [96, 97]. At a national scale, the yield losses of wheat and rice due to $O_3$ in 2015

were projected to be 6.0% and 8.0%, respectively [91]. Zhao et al. [22] recently projected that ground-level $O_3$ during 2015–2018 caused the yield losses of 20.1–33.3% for winter wheat, 5.0–6.3% for maize, and 3.9–8.8% for rice. It should be pointed out here that different yield losses for the same crop may be calculated among different studies, which mainly depends on the definition of the accumulation period and the selection of $O_3$ exposure indicators and corresponding response functions [78]. In recent years, the stomatal $O_3$ flux is regarded as the best indicator for quantifying the potential risks of $O_3$ to crops, mainly because it involves not only $O_3$ concentration but also environmental factors such as temperature, radiation, water vapor pressure difference, and soil moisture content [5]. However, due to the lack of large-scale meteorological observation data, there are relatively few studies on regional-scale $O_3$ risk assessment based on the stomatal $O_3$ flux, and only a few studies are carried out by atmospheric chemistry models and satellite remote sensing methods [37, 86, 88]. To date, only two studies have evaluated crop yield losses caused by $O_3$ exposure in China using concentration- and flux-based indices. A comparison between these two indices indicated that ground-level $O_3$ reduced wheat yields losses of 6.4–7.2% and 10.3–14.9% in 2000 across China based on AOT40 and stomatal $O_3$ flux, respectively [88], whereas in the study by Feng et al. [98], estimates of $O_3$-induced wheat yield reductions for the whole China based on AOT40 were significantly higher

than those based on the stomatal $O_3$ flux. This discrepancy could be explained by the source of data and the choice of dose–response functions [22].

## Limitations and Future Research Directions

Since the 1990s, although a lot of studies on the effects of $O_3$ on crops have been carried out in China, there are still many shortcomings needed to be improved. Therefore, in order to scientifically assess the potential risks of ground-level $O_3$ pollution to crops and provide more valuable information for decision-makers, more in-depth research is needed in the following aspects in the future.

Firstly, previous studies on regional-scale $O_3$ agricultural risk assessment using observational data are usually based on a few monitoring sites, which may affect the accuracy and reliability of the assessment results. Starting from 2013, China has successively established a large number of air quality monitoring stations in almost all cities, and thus, it is possible for researchers to evaluate nationwide $O_3$-induced agricultural losses. It should be noted that although China currently has more than 2000 $O_3$ monitoring stations, their spatial distribution is uneven, and most of the stations are located in urban areas. Studies have shown that the $O_3$ concentration in suburban areas was generally higher than that in urban areas [78]. If $O_3$ in a certain city is used to describe the $O_3$ situation in the planting area of this city, the stress effect of $O_3$ on crops will be underestimated. We should consider building more stations in suburban areas to reduce this uncertainty.

Secondly, the response relationship between crop yield and $O_3$ evaluation index in China established by most of the previous studies is based on OTC experiments. However, climatic factors such as temperature, relative humidity, light, soil moisture, and wind in the OTC chamber are significantly different from the external environmental conditions, which leads to different responses of crops to $O_3$ stress. However, the FACE experiment is regarded as the most appropriate method to investigate the yield responses of crops to elevated $O_3$ [5], because the energy and gas exchange of crop canopy will not be disturbed by the FACE systems. A recent study showed that the sensitivity of wheat and rice to $O_3$ under the OTC experiment was lower than that under the FACE experiment, while it was the opposite for soybeans [99]. Therefore, the results from the OTC experiment cannot be fully applied to the regional $O_3$ risk assessment of natural ecosystems, and experimental research based on the $O_3$-FACE platform should be increased in the future. Meanwhile, different varieties of the same crop have different responses to $O_3$ stress [37, 40, 78]. Future research should consider the impact of varieties and establish the relationship between different varieties of crops and evaluation indicators, which

is beneficial to cultivate crop varieties resistant to $O_3$ and prevent the adverse effects of $O_3$ on crops.

Thirdly, the damage effect of $O_3$ on crops was determined by $O_3$ flux. As a traditional $O_3$ flux observation, the flux chamber method has been widely used due to its simple operation and low cost, while this method changes the growth environment of the crop body and may bring certain errors to the experimental results. The micrometeorological method is an advanced method for measuring the $O_3$ flux of the ecosystem in recent years. This method has already been applied in Europe and America, but it is still relatively few in China, and further research is still needed. In addition, the regional-scale $O_3$ agricultural risk assessments in previous studies were mainly based on the concentration-based indices, because their calculations are quite simple and only use the hourly $O_3$ concentrations. However, the impacts of climate factors have played an important role in the whole crop growth in fact, and the reduced relative yield was the combination of $O_3$ and climate factors. Therefore, the flux-based index, especially the stomatal $O_3$ flux, is regarded as the most scientific indicator. It must be pointed out that the flux-based index depends on too much parameters, and it is difficult to calculate it by using actual observational data. The current air quality models (e.g., WRF-CMAQ) can solve this issue and provide the hourly simulated climate factors and $O_3$ concentration data. In future research, we should consider combining atmospheric chemistry models and satellite remote sensing methods to estimate the distribution of the flux-based indices, which provides an important basis for scientifically quantifying the risk of $O_3$ to crops on a regional scale.

Finally, crop has a certain defensive ability against $O_3$ damage, which will be affected by factors such as crop species, growth period, and environmental conditions. Previous studies only set it as a threshold when calculating the absorption flux of stomata $O_3$ and did not consider its dynamic changes. Therefore, combining the $O_3$ absorption flux model to simulate the detoxification effect of crops is an inevitable trend in future research.

## Declarations

**Conflict of interest** The author declares that he has no conflict of interest.

**Human and Animal Rights** This article does not contain any studies with human or animal subjects performed by any of the authors.

# References

1. Sicard P, Serra R, Rossello P. Spatiotemporal trends in ground-level ozone concentrations and metrics in France over the time period 1999–2012. Environ Res. 2016;149:122–44.

2. Vingarzan R. A review of surface ozone background levels and trends. Atmos Environ. 2014;38:3431–42.

3. Paoletti E. Impact of ozone on Mediterranean forests: a review. Environ Pollut. 2006;144(2):463–74.

4. Zhao H, Zheng Y, Li T, Wei L, Guan Q. Temporal and spatial variation in, and population exposure to, summertime ground-level ozone in Beijing. Int J Environ Res Public Health. 2018;15:628.

5. Feng Z, Tang H, Uddling J, Pleijel H, Kobayashi K, Zhu J, et al. A stomatal ozone flux–response relationship to assess ozone-induced yield loss of winter wheat in subtropical China. Environ Pollut. 2012;164:16–23.

6. Ainsworth EA. Rice production in a changing climate: a meta-analysis of responses to elevated carbon dioxide and elevated ozone concentration. Glob Chang Biol. 2008;14:1642–50.

7. Lombardozzi D, Levis S, Bonan G, Hess PG, Sparks JP. The Influence of chronic ozone exposure on global carbon and water cycles. J Clim. 2015;28(1):292–305.

8. Screpanti A, De Marco A. Corrosion on cultural heritage buildings in Italy: a role for ozone? Environ Pollut. 2009;157(5):1513–20.

9. Fares S, McKay M, Holzinger R, Goldstein AH. Ozone fluxes in a *Pinus ponderosa* ecosystem are dominated by non-stomatal processes: evidence from long-term continuous measurements. Agric For Meteorol. 2010;150:420–31.

10. Avnery S, Mauzerall DL, Liu J, Horowitz LW. Global crop yield reductions due to surface ozone exposure: 2. Year 2030 potential crop production losses and economic damage under two scenarios of O3 pollution. Atmos Environ. 2011;45(13):2297–309.

11. Zhao H, Chen K, Liu Z, Zhang Y, Shao T, Zhang H. Coordinated control of $PM_{2.5}$ and $O_3$ is urgently needed in China after implementation of the "Air pollution prevention and control action plan." Chemosphere. 2021;270:129441.

12. Li K, Jacob DJ, Liao H, Shen L, Zhang Q, Bates KH. Anthropogenic drivers of 2013–2017 trends in summer surface ozone in China. Proc Natl Acad Sci USA. 2019;116:422–7.

13. Tan Z, Hofzumahaus A, Lu K, Brown SS, Holland F, Huey LG, et al. No evidence for a significant impact of heterogeneous chemistry on radical concentrations in the North China Plain in summer 2014. Environ Sci Technol. 2020;54:5973–9.

14. Cai S, Wang Y, Zhao B, Wang S, Chang X, Hao J. The impact of the "Air Pollution Prevention and Control Action Plan" on $PM_{2.5}$ concentrations in Jing-Jin-Ji region during 2012–2020. Sci Total Environ. 2017;580:197–209.

15. Ma Z, Xu J, Quan W, Zhang Z, Lin W, Xu X. Significant increase of surface ozone at a rural site, north of eastern China. Atmos Chem Phys. 2016;16:3969–77.

16. Xu X, Lin W, Wang T, Yan P, Tang J, Meng Z, et al. Long-term trend of surface ozone at a regional background station in eastern China 1991–2006: enhanced variability. Atmos Chem Phys. 2008;8:2595–607.

17. Xu W, Lin W, Xu X, Tang J, Huang J, Wu H, et al. Long-term trends of surface ozone and its influencing factors at the Mt Waliguan GAW station, China- part 1: overall trends and characteristics. Atmos Chem Phys. 2016;16(10):6191–205.

18. Li J, Lu K, Lv W, Li J, Zhong L, Ou Y, et al. Fast increasing of surface ozone concentrations in Pearl River Delta characterized by a regional air quality monitoring network during 2006–2011. J Environ Sci. 2014;26(1):23–36.

19. Song C, He J, Wu L, Jin T, Chen X, Li R, et al. Health burden attributable to ambient $PM_{2.5}$ in China. Environ Pollut. 2017;223:575–86.

20. Wang T, Xue L, Brimblecombe P, Lam YF, Li L, Zhang L. Ozone pollution in China: a review of concentrations, meteorological influences, chemical precursors, and effects. Sci Total Environ. 2017;575:1582–96.

21. Xu L, Batterman S, Chen F, Li J, Zhong X, Feng Y, et al. Spatiotemporal characteristics of $PM_{2.5}$ and PM10 at urban and corresponding background sites in 23 cities in China. Sci Total Environ. 2017;599–600:2074–84.

22. Zhao H, Zheng Y, Zhang Y, Li T. Evaluating the effects of surface $O_3$ on three main food crops across China during 2015–2018. Environ Pollut. 2020;258:113794.

23. Tie X, Geng F, Guenther A, Cao J, Greenberg J, Zhang R, et al. Megacity impacts on regional ozone formation: observations and WRF-Chem modeling for the MIRAGE-Shanghai field campaign. Atmos Chem Phys. 2013;13:5655–69.

24. Tang G, Wang Y, Li X, Ji D, Hsu S, Gao X. Spatial-temporal variations in surface ozone in Northern China as observed during 2009–2010 and possible implications for future air quality control strategies. Atmos Chem Phys. 2012;12:2757–76.

25. Gligorovski S, Strekowski R, Barbati S, Vione D. Environmental implications of hydroxyl radicals (•OH). Chem Rev. 2015;115(24):13051–92.

26. Zhang J, An J, Qu Y, Liu X, Chen Y. Impacts of potential HONO sources on the concentrations of oxidants and secondary organic aerosols in the Beijing-Tianjin-Hebei region of China. Sci Total Environ. 2019;647:836–52.

27. Piikki K, Temmerman LD, Pleijel H. The open-top chamber impact on vapour pressure deficit and its consequences for stomatal ozone uptake. Atmos Environ. 2008;42(26):6513–22.

28. Pleijel H, Broberg MC, Uddling J. Ozone impact on wheat in Europe, Asia and North America-a comparison. Sci Total Environ. 2019;664:908–14.

29. Pleijel H, Danielsson H, Emberson L, Ashmore MR, Mills G. Ozone risk assessment for agricultural crops in Europe: further development of stomatal flux and flux–response relationships for European wheat and potato. Atmos Environ. 2007;41(14):3022–40.

30. Mills G, Pleijel H, Braun S, Büker P, Bermejo V, Calvo E, et al. New stomatal flux-based critical levels for ozone effects on vegetation. Atmos Environ. 2011;45(28):5064–8.

31. Wu R, Zheng Y, Hu C. Evaluation of the chronic effects of ozone on biomass loss of winter wheat based on ozone flux-response relationship with dynamical flux thresholds. Atmos Environ. 2016;142:93–103.

32. Gerosa G, Marzuoli R, Desotgiu R, Bussotti F, Ballarin-Denti A. Visible leaf injury in young trees of *Fagus sylvatica* L. and *Quercus robur* L. in relation to ozone uptake and ozone exposure. An open-top chambers experiment in South Alpine environmental conditions. Environ Pollut. 2008;152(2):274–84.

33. Emberson LD, Büker P, Ashmore MR, Mills G, Jackson LS, Agrawal M, et al. A comparison of North American and Asian exposure response data or ozone effects on crop yields. Atmos Environ. 2009;43(12):1945–53.

34. Ghosh A, Agrawal M, Agrawal SB. Effect of water deficit stress on an Indian wheat cultivar (*Triticum aestivum* L. HD 2967) under ambient and elevated level of ozone. Sci Total Environ. 2020;714:136837.

35. Danielsson H, Karlsson GP, Karlsson PE, Pleijel H. Ozone uptake modelling and flux-response relationships—an assessment of ozone-induced yield loss in spring wheat. Atmos Environ. 2003;37(4):475–85.

36. Hoshika Y, Katata G, Deushi M, Watanabe M, Koike T, Paoletti E. Ozoneinduced stomatal sluggishness changes carbon and water balance of temperate deciduous forests. Sci Rep. 2015;5:9871.

37. Mills G, Sharps K, Simpson D, Pleijel H, Broberg M, Uddling J, et al. Ozone pollution will compromise efforts to increase global wheat production. Glob Chang Biol. 2018;24:3560–74.

38. Zhu ZL, Sun XM, Yu GR, Wen XF. A review of research on ozone flux observation and stomatal uptake estimation over terrestrial ecosystems. Acta Ecol Sin. 2014;34(31):6029–38 (in Chinese).

39. Tong L, Wang XK, Sudebilige, Wang Q, Geng CM, Wang W, et al. Stomatal ozone uptake modeling and comparative analysis of flux-response relationships of rice. J Agro-Environ. 2011;30(10):1930–8 (in Chinese).

40. Feng Z, Tang H, Uddling J, Pleijel H, Kobayashi K, Zhu J, et al. A stomatal ozone flux–response relationship to assess ozone-induced yield loss of winter wheat in subtropical China. Environ Pollut. 2012;164(1):16–23.

41. Tong L, Feng ZW, Sudebilige, Wang Q, Geng CM, Lu F, et al. Stomatal ozone uptake modeling and comparative analysis of flux-response relationships of winter wheat. Acta Ecol Sin. 2012;32(9):2890–9 (in Chinese).

42. Zhang W, Feng Z, Wang X, Liu X, Hu E. Quantification of ozone exposure-and stomatal uptake- yield response relationships for soybean in Northeast China. Sci Total Environ. 2017;599–600:710–20.

43. Pleijel H, Danielsson H, Ojanperä K, Temmerman LD, Högy P, Badiani M, et al. Relationships between ozone exposure and yield loss in European wheat and potato—a comparison of concentration- and flux-based exposure indices. Atmos Environ. 2004;38(15):2259–69.

44. Karlsson P, Braun S, Broadmeadow M, Elvira S, Emberson L, Gimeno BS, et al. Risk assessments for forest trees: the performance of the ozone flux versus the AOT concepts. Environ Pollut. 2007;146(3):608–16.

45. Goumenaki E, Fernandez IG, Papanikolaou A, Papadopoulou A, Askianakis C, Kouvarakis G, et al. Derivation of ozone flux-yield relationships for lettuce: a key horticultural crop. Environ Pollut. 2007;146(3):699–706.

46. Gonzalez-Fernandez I, Kaminska A, Dodmani M, Goumenaki E, Quarrie S, Barnes JD. Establishing ozone flux–response relationships for winter wheat: analysis of uncertainties based on data for UK and Polish genotypes. Atmos Environ. 2010;44(5):621–30.

47. Breuninger C, Oswald R, Kesselmeier J, Meixner FX. The dynamic chamber method: trace gas exchange fluxes (NO, $NO_2$, $O_3$) between plants and the atmosphere in the laboratory and in the field. Atmos Meas Tech. 2012;5:955–89.

48. Wu ZY, Zhang L, Wang XM, Munger JW. A modified micrometeorological gradient method for estimating $O_3$ dry depositions over a forest canopy. Atmos Chem Phys. 2015;15:7487–96.

49. Fares S, McKay M, Holzinger R, Goldstein AH. Ozone fluxes in a Pinus ponderosa ecosystem are dominated by non-stomatal processes: evidence from long-term continuous measurements. Agric For Meteorol. 2010;150(3):420–31.

50. Fowler D, Pilegaard K, Sutton MA, Ambus P, Raivonen M, Duyzer J, et al. Atmospheric composition change: ecosystems–atmosphere interactions. Atmos Environ. 2009;43(33):5193–267.

51. Altimir N, Tuovinen JP, Vesala T, Kulmala M, Hari P. Measurements of ozone removal by Scots pine shoots: calibration of a stomatal uptake model including the non-stomatal component. Atmos Environ. 2004;38(15):2387–98.

52. Altimir N, Kolari P, Tuovinen JP, Vesala T, Bäck J, Suni T, et al. Foliage surface ozone deposition: a role for surface moisture? Biogeosciences. 2006;2:209–28.

53. Launiainen S, Katul GG, Grönholm T, Vesala T. Partitioning ozone fluxes between canopy and forest floor by measurements and a multi-layer model. Agric For Meteorol. 2013;173:85–99.

54. Coyle M, Nemitz E, Storeton-West R, Fowler D, Cape JN. Measurements of ozone deposition to a potato canopy. Agric For Meteorol. 2009;149:655–66.

55. Gerosa G, Finco A, Mereu S, Vitale M, Manes F, Denti AB. Comparison of seasonal variations of ozone exposure and fluxes in a Mediterranean Holm oak forest between the exceptionally dry 2003 and the following year. Environ Pollut. 2009;157(5):1737–44.

56. Zhang L, Vet R, Brook JR, Legge AH. Factors affecting stomatal uptake of ozone by different canopies and a comparison between dose and exposure. Sci Total Environ. 2006;370(1):117–32.

57. Liu Z, Pan Y, Song T, Hu B, Wang L, Wang Y. Eddy covariance measurements of ozone flux above and below a southern subtropical forest canopy. Sci Total Environ. 2021;791:148338.

58. Vitale M, Gerosa G, Ballarin-Denti A, Manes F. Ozone uptake by an evergreen Mediterranean forest (*Quercus ilex* L.) in Italy-part II: flux modelling. Upscaling leaf to canopy ozone uptake by a process-based model. Atmos Environ. 2005;39:3267–78.

59. Matsuda K, Watanabe I, Wingpud V, Theramongkol P, Ohizumi T. Deposition velocity of $O_3$ and $SO_2$ in the dry and wet season above a tropical forest in northern Thailand. Atmos Environ. 2006;40:7557–64.

60. Zhang L, Brook JR, Vet R. On ozone dry deposition-with emphasis on non-stomatal uptake and wet canopies. Atmos Environ. 2002;36:4787–99.

61. Matsuda K, Watanabe I, Wingpud V, Theramongkol P, Ohizumi T. Deposition velocity of $O_3$ and $SO_2$ in the dry and wet season above a tropical forest in northern Thailand. Atmos Environ. 2006;40(39):7557–64.

62. Sorimachi A, Sakamoto K, Ishihara H, Fukuyama T, Utiyama M, Liu H, et al. Measurements of sulfur dioxide and ozone dry deposition over short vegetation in northern China-a preliminary study. Atmos Environ. 2003;37:3157–66.

63. Lamaud E, Carrara A, Brunet Y, Lopez A, Druilhet A. Ozone fluxes above and within a pine forest canopy in dry and wet conditions. Atmos Environ. 2002;36(1):77–88.

64. Kurpius MR, McKay M, Goldstein AH. Annual ozone deposition to a Sierra Nevada ponderosa pine plantation. Atmos Environ. 2002;36:4503–15.

65. Zhu ZL, Sun XM, Dong YS, Zhao FH, Meixner FX. Diurnal variation of ozone flux over corn field in Northwestern Shandong Plain of China. Sci China Earth Sci. 2014;57:503–11.

66. Rannik Ü, Altimir N, Mammarella I, Bäck J, Rinne J, Ruuskanen TM, et al. Ozone deposition into a boreal forest over a decade of observations: evaluating deposition partitioning and driving variables. Atmos Chem Phys. 2012;12:12165–82.

67. Pan XL, Wang ZF, Wang XQ, Dong HB, Xie FY, Guo YH. An observation study of ozone dry deposition over grassland in the suburban area of Beijing. Atmos Sci. 2010;34(1):1200–2130 (in Chinese).

68. Li S, Zheng YF, Wu RJ, Yin JF, Xu JX, Zhao H, Sun J. Observation of ozone dry deposition in the field of winter wheat. Chin J Appl Ecol. 2016;27(6):1811–9 (in Chinese).

69. Huang JQ, Zheng YF, Xu JX, Zhao H, Yuan Y, Chu ZF. $O_3$ dry deposition flux observation and soil resistance modeling over a bare soil in Nanjing area in autumn. Chin J Appl Ecol. 2016;27(10):3196–204 (in Chinese).

70. Zhao H, Zheng YF, Li S, Yuan Y, Huang JQ, Liu J, Cao JC. Observation and simulation of $CO_2$ and $O_3$ fluxes in the winter wheat field based on micrometeorological method. China Environ Sci. 2020;40(3):1038–48.

71. Lamaud E, Loubet B, Irvine M, Stella P, Personne E, Cellier P. Partitioning of ozone deposition over a developed maize crop between stomatal and non-stomatal uptakes, using eddy-covariance flux measurements and modelling. Agric For Meteorol. 2009;149:1385–96.

72. Stella P, Personne E, Lamaud E, Loubet B, Trebs I, Cellier P. Assessment of the total, stomatal, cuticular, and soil 2 year

ozone budgets of an agricultural field with winter wheat and maize crops. JGR Biogeosci. 2013;118:1–13.

73. Stella P, Personne E, Loubet B, Lamaud E, Cellier P, Beziat P, et al. Predicting and partitioning ozone fluxes to maize crops from sowing to harvest: the Surfatm-O3 model. Biogeosciences. 2011;8:2869–86.

74. Xu JX, Zheng YF, Zhao H, Chu ZF, Huang JQ, Yuan Y. Ozone deposition and risk assessment for a winter wheat field: partitioning between stomatal and non-stomatal pathways. Environ Sci. 2017;38(10):4427–37 (in Chinese).

75. Cieslik S. Ozone fluxes over various plant ecosystems in Italy: a review. Environ Pollut. 2009;157(5):1487–96.

76. Gerosa G, Marzuoli R, Cieslik S, Ballarin-Denti A. Stomatal ozone fluxes over a barley field in Italy. "Effective exposure" as a possible link between exposure- and flux-based approaches. Atmos Environ. 2004;38(15):2421–32.

77. Zhao H, Wang SY, Zhang YX, Liu Z, Zheng YF. Ozone dry deposition characteristics and its contribution to stomatal absorption in a paddy ecosystem. China Environ Sci. 2021;41(7):3298 (in Chinese).

78. Zhao H, Zheng Y, Wu X. Assessment of yield and economic losses for wheat and rice due to ground-level O3 exposure in the Yangtze River Delta. China Atmos Environ. 2018;191:241–8.

79. Feng Z, Jin M, Zhang F, Huang Y. Effects of ground-level ozone (O3) pollution on the yields of rice and winter wheat in the Yangtze River Delta. J Environ Sci. 2003;15(3):360–2.

80. Wang X, Zhang Q, Zheng F, Zheng Q, Yao F, Chen Z, et al. Effects of elevated O3 concentration on winter wheat and rice yields in the Yangtze River Delta. China Environ Pollut. 2012;171(1):118–25.

81. Xie JQ, Zheng QW, Wang XK, Zhang BJ. Effect of ozone on photosynthesis of rice leaves, ear character and yield component in situe. Acta Agric Boreali-Occident Sin. 2006;15(3):27–30.

82. Pang J, Kobayashi K, Zhu JG. Yield and photosynthetic characteristics of flag leaves in Chinese rice (Oryza sativa L.) varieties subjected to free-air release of ozone. Agric Ecosyst Environ. 2009;132(3–4):203–11.

83. Zhang JS, Tang HY, Liu G, Zhu JG. Stomatal ozone fluxresponse relationships of rice (Oryza sativa L.) in subtropical area. J Agro-Environ Sci. 2016;35(10):1857–66.

84. Peng J, Shang B, Xu Y, Feng Z, Pleijel H, Calatayud V. Ozone exposure- and flux-yield response relationships for maize. Environ Pollut. 2019;252:1–7.

85. Van Dingenen R, Dentener FJ, Raes F, Krol MC, Emberson L, Cofala J. The global impact of ozone on agricultural crop yields under current and future air quality legislation. Atmos Environ. 2009;43:604–18.

86. Fishman J, Creilson JK, Parker PA, Ainsworth EA, Vining GG, Szarka J, et al. An investigation of widespread ozone damage to the soybean crop in the upper Midwest determined from ground-based and satellite measurements. Atmos Environ. 2010;44(18):2248–56.

87. Li P, Marco AD, Feng ZZ, Anav A, Zhou D, Paoletti E. Nationwide groundlevel ozone measurements in China suggest serious risks to forests. Environ Pollut. 2018;237:803–13.

88. Tang H, Takigawa M, Liu G, Zhu J, Kobayashi K. A projection of ozone-induced wheat production loss in China and India for the years 2000 and 2020 with exposure-based and flux-based approaches. Glob Change Biol. 2013;19(9):2739–52.

89. Liu F, Wang X, Zhu Y. Assessing current and future ozone-induced yield reductions for rice and winter wheat in Chongqing and the Yangtze River Delta of China. Environ Pollut. 2009;157(2):707–9.

90. Zhu Z, Sun X, Zhao F, Meixner FX. Ozone concentrations, flux and potential effect on yield during wheat growth in the Northwest-Shandong plain of China. J Environ Sci. 2015;34(8):1–9.

91. Feng Z, De Marco A, Anav A, Gualtieri M, Sicard P, Tian H, et al. Economic losses due to ozone impacts on human health, forest productivity and crop yield across China. Environ Int. 2019;131:104966.

92. Lin Y, Jiang F, Zhao J, Zhu G, He X, Ma X, et al. Impacts of O3 on premature mortality and crop yield loss across China. Atmos Environ. 2018;194:41–7.

93. Tang H, Pang J, Zhang G, Takigawa M, Liu G, Zhu J. Mapping ozone risks for rice in China for years 2000 and 2020 with flux-based and exposure-based doses. Atmos Environ. 2014;86:74–83.

94. Ren X, Shang B, Feng Z, Calatayud V. Yield and economic losses of winter wheat and rice due to ozone in the Yangtze River Delta during 2014–2019. Sci Total Environ. 2020;745:140847.

95. Cao J, Wang X, Zhao H, Ma M, Chang M. Evaluating the effects of ground-level O3 on rice yield and economic losses in Southern China. Environ Pollut. 2020;267:115694.

96. Hu T, Liu S, Xu Y, Feng Z, Calatayud V. Assessment of O3-induced yield and economic losses for wheat in the North China Plain from 2014 to 2017. China Environ Pollut. 2020;258:113828.

97. Feng Z, Hu T, Tai APK, Calatayud V. Yield and economic losses in maize caused by ambient ozone in the North China Plain (2014–2017). Sci Total Environ. 2020;722:137958.

98. Feng Z, Kobayashi K, Li P, Xu Y, Tang H, Guo A, et al. Impacts of current ozone pollution on wheat yield in China as estimated with observed ozone, meteorology and day of flowering. Atmos Environ. 2017;217:116945.

99. Feng Z, Uddling J, Tang H, Zhu J, Kobayashi K. Comparison of crop yield sensitivity to ozone between open-top chamber and free-air experiments. Glob Chang Biol. 2018;24:2231–8.